Supporting Information

Impact of Chiral Supramolecular Nanostructure on the Mechanical and Electrical Performances of Triphenylene-based discotic physical gels

*Hongli Zhang, Junjie Cheng, Qiang Zhou, Qijin Zhang, Gang Zou**

Author Affiliations
CAS Key Laboratory of Soft Matter Chemistry, Department of Polymer Science and Engineering, iChEM, University of Science and Technology of China, Hefei, Anhui 230026, P.R.China.

*Corresponding author. Email: gangzou@ustc.edu.cn

Experimental Section

Synthesis of Hexadeca-5,7-diynoic acid 2-azido-ethyl ester (HAD-A)

HAD (248.36 mg, 1 mmol), 2-Azidoethanol (113.21mg, 1.3 mmol), DCC (247.59mg, 1.2 mmol), and DMAP (12.2 mg, 0.1 mmol) were dissolved in 30 mL dry DCM. The reaction mixture was stirred at 30 °C for 24 h under nitrogen atmosphere. After removing the solvent, the residue was extracted with DCM and saturated brines three times, and the organic layer was dried over anhydrous MgSO$_4$. After removing the solvent by rotary evaporator, the crude product was purified by silica gel column chromatography (Hexane: DCM, 1: 1) to yield a white solid.

Synthesis of triazole-modified triphenylene derivative HDATTP

2,3,6,7,10,11-hexakis(pro-2-ynyloxy)triphenylene (55.24mg, 0.1 mmol), HAD-A (258.89mg, 0.8 mmol), (+)-sodium L-ascorbate (67.36 mg, 0.34 mmol), CuSO4$\cdot$5H$_2$O (42.45 mg, 0.17 mmol) were dissolved in 20 mL of THF and 5 mL of deionized water. The reaction mixture was stirred for 12 hours at room temperature. The solvent was removed by a rotary evaporator, and the resulting mixture was extracted with dichloromethane and deionized water three times, and then dried over MgSO$_4$. The dichloromethane was removed in rotary evaporator, and the remaining azido compound was removed by a silica gel column chromatography using dichloromethane: ethyl acetate = 1:1 as the eluent, to yield a brown solid.

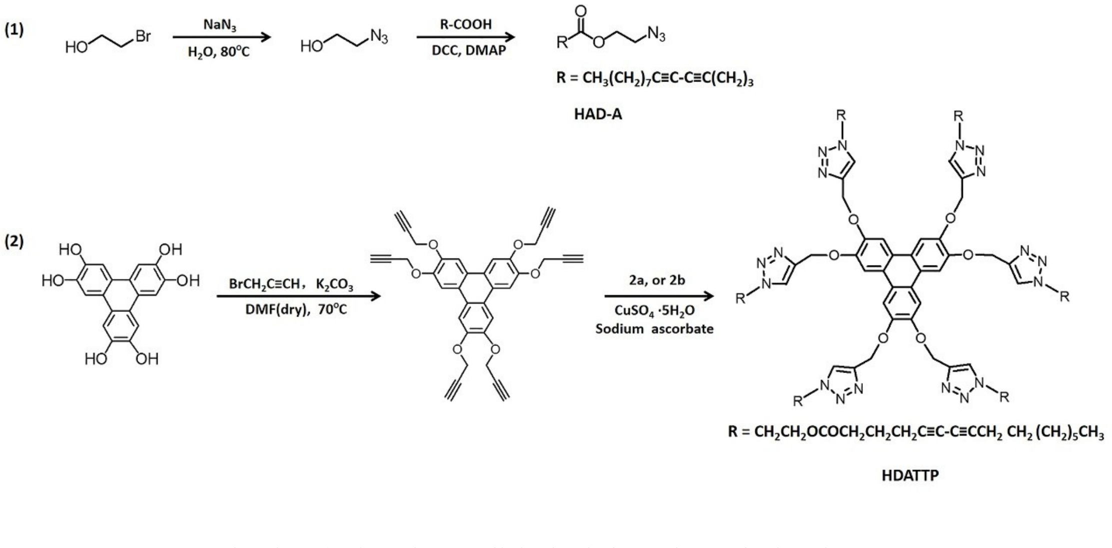

Figure S1. Synthesis of triazole modified triphenylene derivative **HDATTP**.

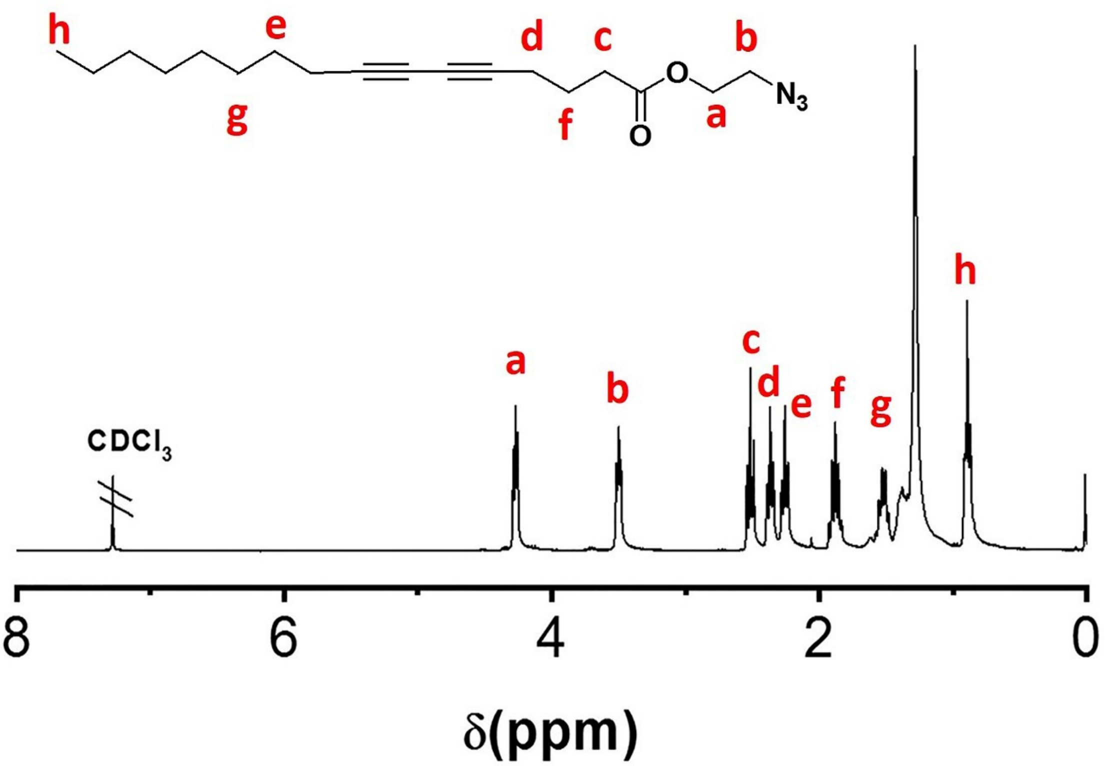

Figure S2. ^{1}H-NMR spectrum of HAD-A.

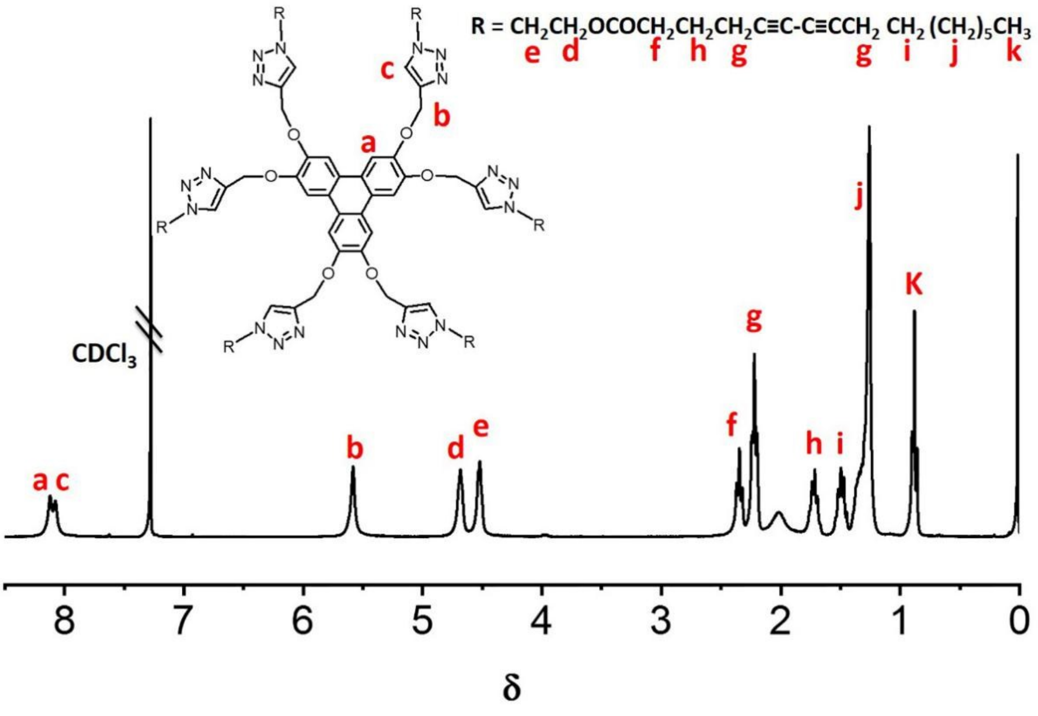

Figure S3. ^{1}H-NMR spectrum of HDATTP.

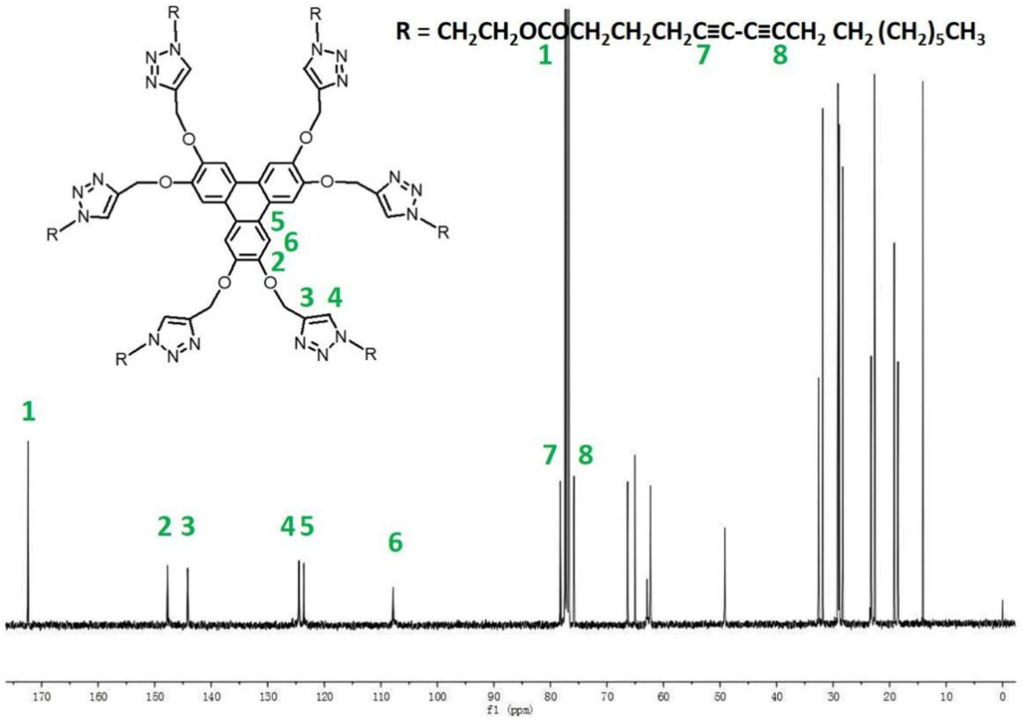

Figure S4. ^{13}C-NMR spectrum of HDATTP.

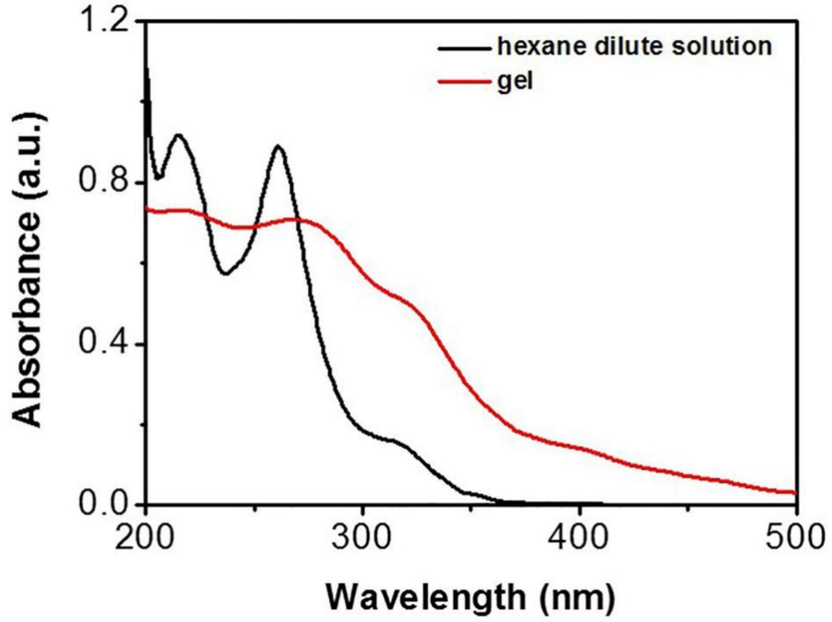

Figure S5. The UV-Vis spectrum of the HDATTP supramolecular gel (red line) and the dilute solution in hexane (black line).

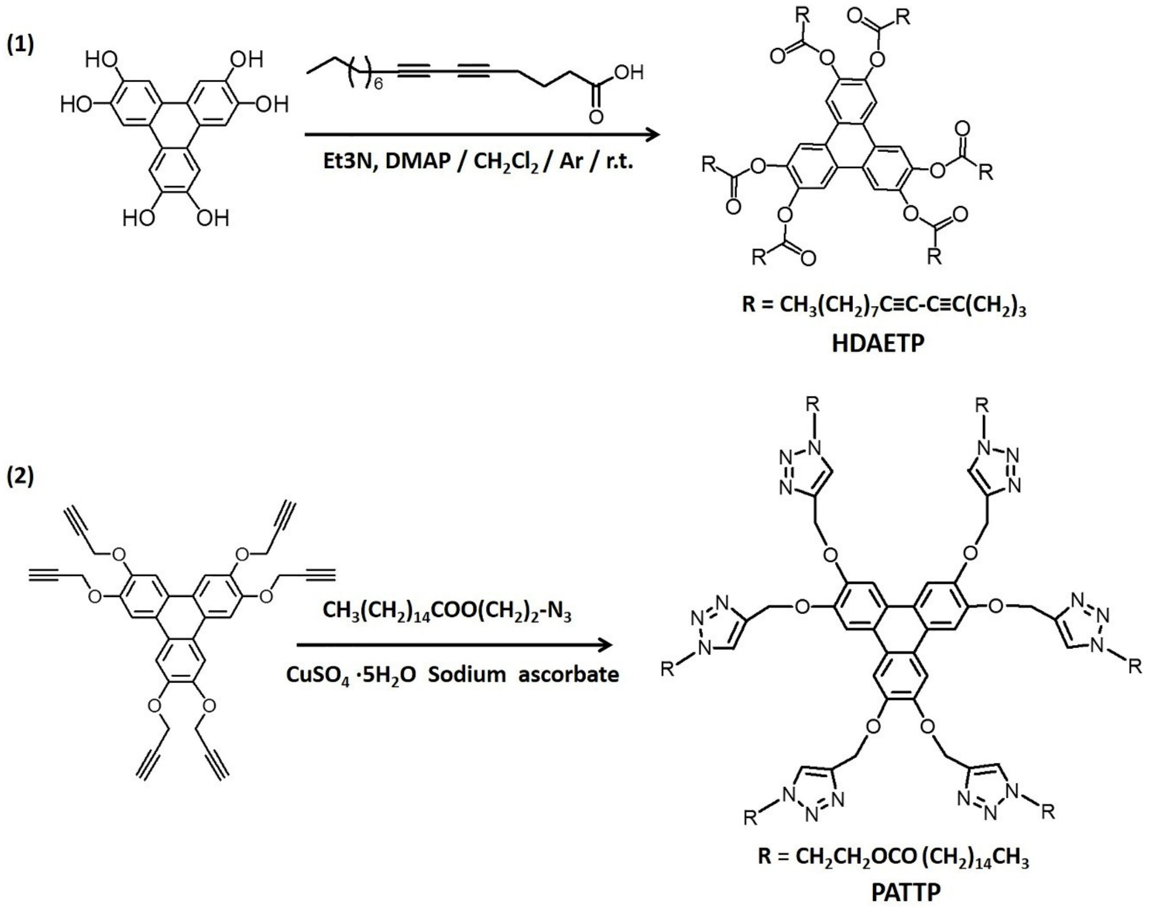

Figure S6. Synthetic routes and the molecular structures of HDAETP and PATTP.

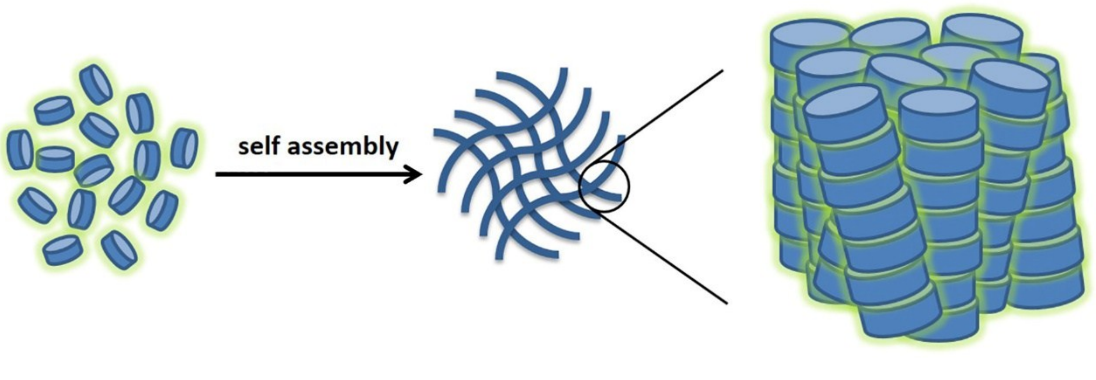

Figure S7. Schematic illumination of supramolecular assembly process for achiral HDATTP in low polar solvents.

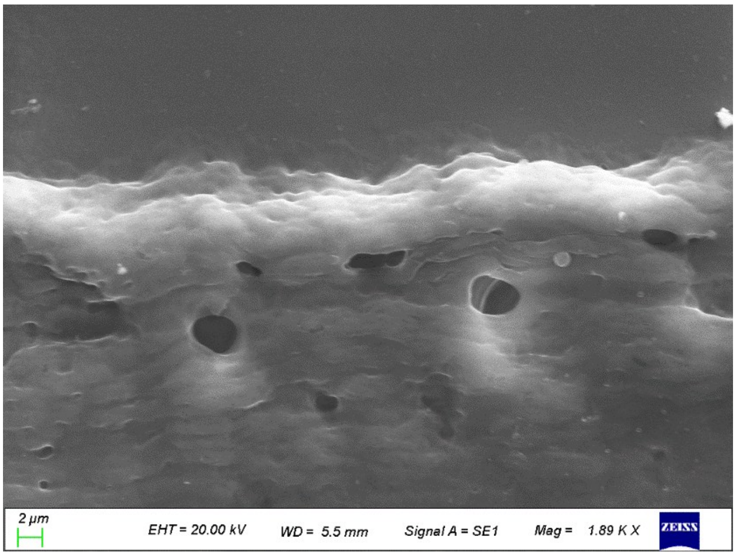

Figure S8. SEM image of the supramolecular gel of HDATTP.

Table S1. Gelation property of HDATTP in different solvents.

Entry	Solvent	Gelation property
1	DMF	Solution
2	DCM	Solution
3	THF	Solution
4	limonene	Solution
5	cyclohexane	Gel
6	hexane	Gel
7	cyclohexane/ hexane=1:1	Gel
8	limonene/ hexane=1:10	Gel

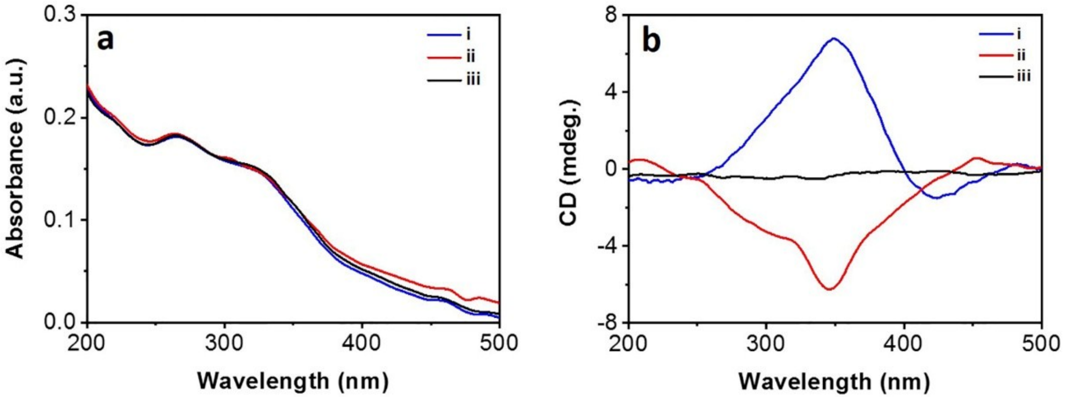

Figure S9. (a) UV-Vis and (b) CD spectra of the HDATTP xerogel.

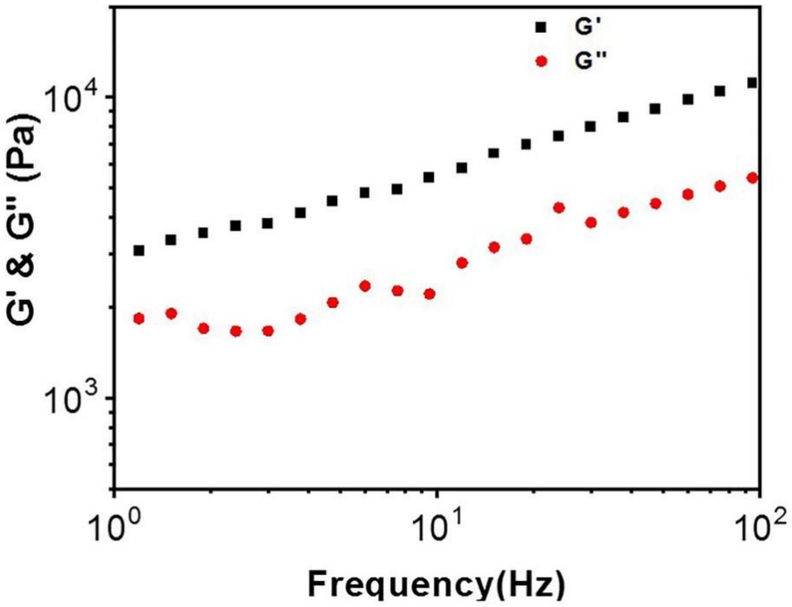

Figure S10. Frequency-sweep measurements of M-helix nanostructure supramolecular gels.

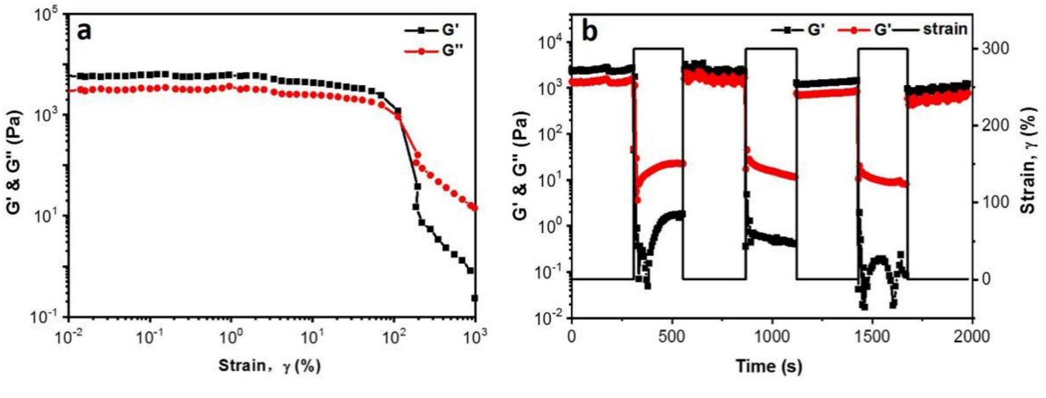

Figure S11. (a) Stress sweep experiments and (b) repeated dynamic strain step tests of M-helix nanostructure supramolecular gel.

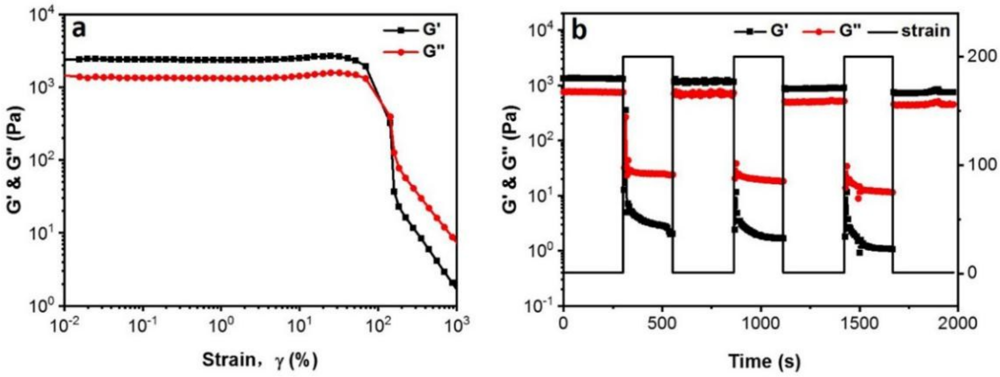

Figure S12. (a) Stress sweep experiments and (b) repeated dynamic strain step tests of racemic supramolecular gel.

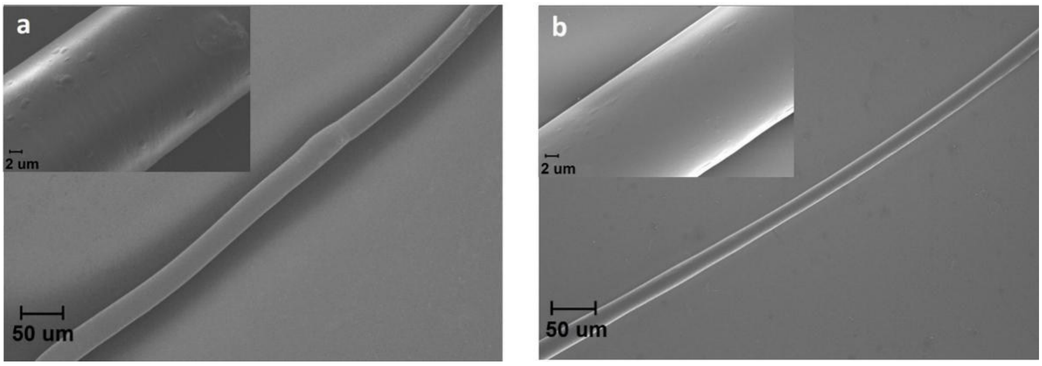

Figure S13. SEM images of single microfiber manual stretched from (a) M-helix and (b) racemic supramolecular gels (inset: magnified SEM images of that supramolecular gel microfibers).

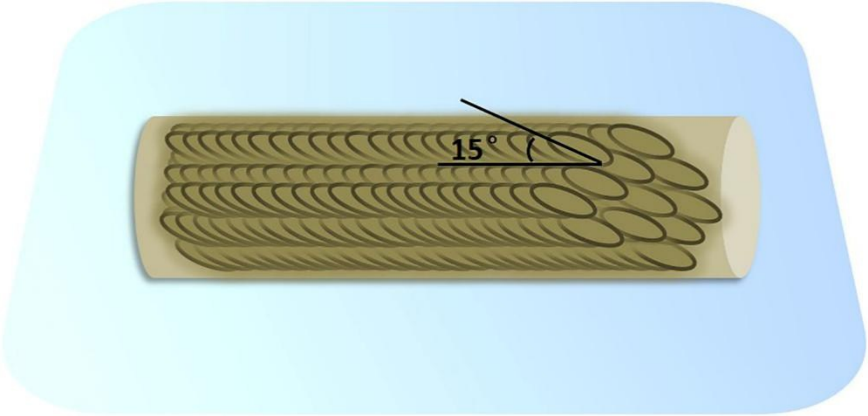

Figure S14. Scheme of the orientation of the discotic molecular in the microfiber.

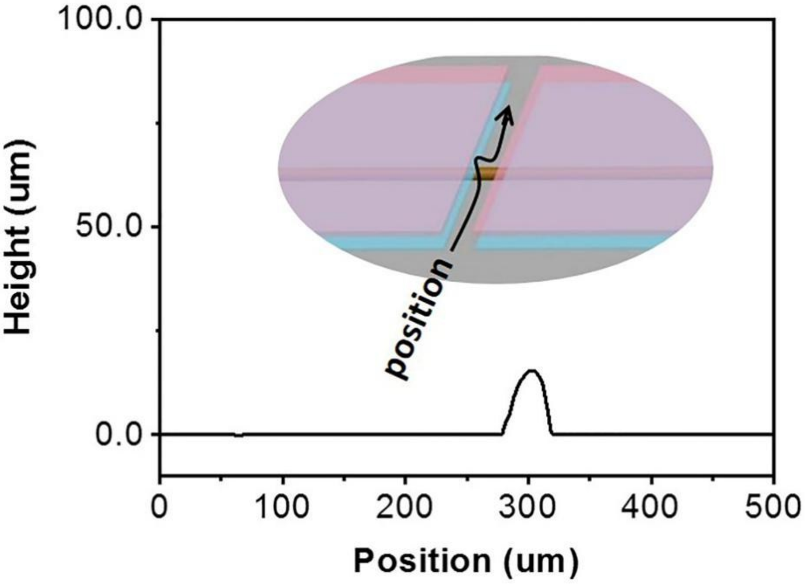

Figure S15. The typical step profiler analysis for determination of the cross-sectional area of the microfiber.